15TH IEA HEAT PUMP CONFERENCE
MAY 26–29, 2026 | HOFBURG
VIENNA 2026
DECARBONISATION THROUGH INNOVATION

Exploring the mutual relationship between heat pumps and Urban Heat Islands via building simulation

Chiara Martone[a], Giovanna Pallotta[a], Ilenia Perugini[a],
Maurizio Sasso[a*], Luca Ventola[a]

[a]University of Sannio, Department of Engineering, Benevento, Italy

Abstract

Rising temperatures, a key consequence of climate change, are driving increased cooling demands, which in turn lead to higher greenhouse gas emissions, particularly when relying on fossil fuel-based power supply. While direct emissions from heat pumps are projected to decrease with the adoption of low global warming potential refrigerants, and increased energy consumption might be balanced by renewable energy sources, the widespread use of these systems has also a significant, and often neglected, local environmental impact. In dense cities, the thermal energy discharged by condensers exacerbates urban heat islands (UHI) phenomena, which can have substantial negative effects on human health. This study investigates the mutual relationship between heat pump technology and UHI through an empirical analysis grounded in building energy simulation. A real building located in Southern Italy is analyzed to assess the impact of UHI-induced temperature variations on heat pump performance in both heating and cooling modes. This includes quantifying changes in energy consumption, performance, and evolving users' behavior in different scenarios. The environmental impact is evaluated through the Expanded Total Equivalent Warming Impact, an index specifically developed to improve traditional assessments by accounting for UHI phenomena. The results demonstrate how even a slight increase in external temperature can significantly alter the building's energy requirements: while UHI phenomena decrease energy consumption in winter, cooling demand is projected to increase rapidly. The findings of this analysis highlight the growing influence of UHI phenomena on the heating, ventilation, air conditioning, and refrigeration sector, providing valuable insights into its complex interactions with the adoption of heat pumps. This research offers crucial information for urban planners, building designers, and policymakers seeking to optimize building energy efficiency and mitigate the adverse health effects of rising temperatures.

Keywords: Climate Change; Electric Heat Pump; Expanded Total Equivalent Warming Impact; Urban Heat Island..

1. Introduction

According to Buster et al. [1], approximately 1% to 3% of the Earth's surface is classified as urban. Despite occupying a small area, this urbanized region is home to about 55% of the global population, a figure that has grown from 30% in 1950 and is projected to reach 68% by 2050 [2]. This trend contributes to changes in per-capita consumption of various materials and energy resources, as well as to regional and local warming [3], [4]. In this regard, one well-known phenomenon is the urban heat island (UHI) effect, which causes surface and air temperatures in urban areas to be higher than in surrounding rural areas [5], [6]. This issue not only worsens air quality but also increases the energy demand for cooling in buildings, reduces the effectiveness of natural ventilation, and complicates efforts to mitigate global warming [7], [8].

Electric-driven heat pumps (EHPs) are regarded as one of the key technologies for achieving sustainability targets in cities, particularly when powered by renewable-based electric energy production plants [9]. EHPs in buildings can utilize various heat sources; however, air-source heat pumps are the most deployed type [10]. According to data reported by the Joint Research Centre, 23 million EHPs have been installed in the European

Union by 2024 [11]. Air-to-water heat pumps have experienced the fastest growth over the past two decades, with sales increasing by 275% between 2015 and 2024. In contrast, ground- and water-source heat pumps have grown much more slowly, with sales rising by only about 10%. Air-to-air heat pumps have also seen substantial growth, with 827000 units installed in 2024, compared to 87000 units for ground and water-based solutions. The rise in air temperature caused by the UHI effect impacts the performance of these systems in summer and, as a result, increases their electric load [12], [13]. In addition, the condensers of air-source heat pumps operating in cooling mode release heat into the environment, further aggravating the UHI phenomenon [14]. Numerous studies in scientific literature have emphasized the need to mitigate UHI effects by reducing energy consumption in buildings [15], incorporating them into building energy modeling [16], and exploring the interaction between energy system behavior and environmental impact [17]. However, the traditional indexes adopted for the environmental impact assessment of EHPs usually overlook the UHI phenomenon. For instance, the Total Equivalent Warming Impact (TEWI) index accounts for greenhouse gas emissions due to refrigerant leakages into the atmosphere (direct emissions) and those resulting from the operation of the plant (indirect emissions) [18]. Another index, the Life Cycle Climate Performance (LCCP), also considers emissions occurring during the construction and disposal phases of the plant, in addition to those from operation [19]. Although this index considers the reduction in performance of EHPs operating in cooling mode resulting from climate change, it does not account for other factors that are nonetheless relevant to their environmental impact.

To further broaden the scope of environmental impact analysis for EHPs, Ceglia et al. [20] proposed in 2021 a revision of the TEWI index known as the Expanded Total Equivalent Warming Impact (ETEWI). This indicator calculates the direct and indirect contributions already included in TEWI with improved temporal accuracy. Specifically, the direct contribution is determined on a monthly basis and by also accounting for maintenance operations. Moreover, compared to TEWI and LCCP, ETEWI introduces additional sources of greenhouse gas emissions, including:

- the direct and indirect contributions of the UHI effect;
- the indirect contribution from transmission and distribution losses along the natural gas pipeline supplying natural gas-fired power plants;
- the direct contribution from fuel combustion in combustion-based plants, such as those used for domestic hot water production.

ETEWI index was later applied by Ceglia et al. [21] in 2023 to assess the environmental impact of an EHP installed in a university building in southern Italy, revealing notable discrepancies compared to results obtained using the TEWI index. In the present work, the same case study is examined using a simulation-based approach that considers increasing temperature trends. The objective is to assess the impact of global warming on the building's heating and cooling loads, as well as on EHP performance. The environmental impact of the system is then evaluated using the ETEWI index to quantify the increasing effects of the UHI phenomenon. In this context, this study aims to provide a comprehensive environmental assessment of EHP operation under evolving climatic conditions, explicitly incorporating the influence of microclimatic phenomena anticipated to become more pronounced in the coming decades.

2. Methods

In this section the case study and the methods adopted for the environmental impact assessment are introduced.

2.1. User-plant system

The case study focuses on a university building. The structure is a historic facility located in Benevento, in southern Italy, and accommodates offices, laboratories, and classrooms. It features a rectangular layout distributed over three floors, each covering an area of 606.8 m^2, with a total height of 13.0 m. The surface-to-volume ratio of the building is 0.46 m^{-1}. The main thermal and physical properties of both the opaque and transparent envelope components are summarized in Table 1. According to the Italian regulation, Benevento falls within climate zone C, being characterized by 1034 heating degree days [22]. Consequently, the heating season extends from mid-November to the end of March, while the cooling season generally spans from mid-June to late September. The setpoint temperature for indoor conditions is 20°C during heating and 26°C during cooling.

Table 1. Characterization of the building envelope.

Element	Thermal transmittance [W/m²/K]	Thickness [m]	Solar factor [-]
External wall	0.74	0.64	-
Ground floor	2.71	0.46	-
Ceiling	2.60	0.26	-
Roof	1.36	0.35	-
Window	5.86	-	0.48

The air-to-water EHP that supplies the building's space heating and cooling needs is installed on the rooftop. The system's nominal thermal, cooling, and electric power, along with its rated energy efficiency ratio (EER) and coefficient of performance (COP), are summarized in Table 2 [23]. These values refer to input/output water temperatures of 12 and 7°C, respectively, in cooling mode, and of 40 and 45°C, respectively, in heating mode. The EHP operates with R410A as the refrigerant, with a nominal charge of 76 kg.

The plant includes a 750 L thermal storage tank and three circulation pumps with a total electric power of 6.96 kW. Within the building, heating and cooling loads are served by fan coils, whose operation is regulated by room thermostats.

Table 2. Technical parameters of the EHP.

Nominal parameter	Cooling mode	Heating mode
Cooling/thermal power [kW]	230.7	293.5
Electric power [kW]	107.9	94.6
EER/COP [-]	2.14	3.10

2.2. Modelling and simulation

The building-plant system is modelled and simulated using the dynamic software TRNSYS 18 [24]. The building model, shown in Figure 1, is composed of fifteen thermal zones, outlined according to the function and orientation of each space. On the ground floor, three zones are defined: two for classrooms and laboratories and one encompassing the stairwells. The classroom and laboratory zones correspond to the building's right and left wings, facing West and East, respectively. The first floor contains five thermal zones, including two for offices, two for corridors, and one unconditioned area comprising bathrooms and staircases. The top floor mirrors the layout of the first floor, with two office zones and two corridor zones. The unconditioned space, which includes bathrooms and stairwells, is split into three separate thermal zones due to the presence of an internal terrace.

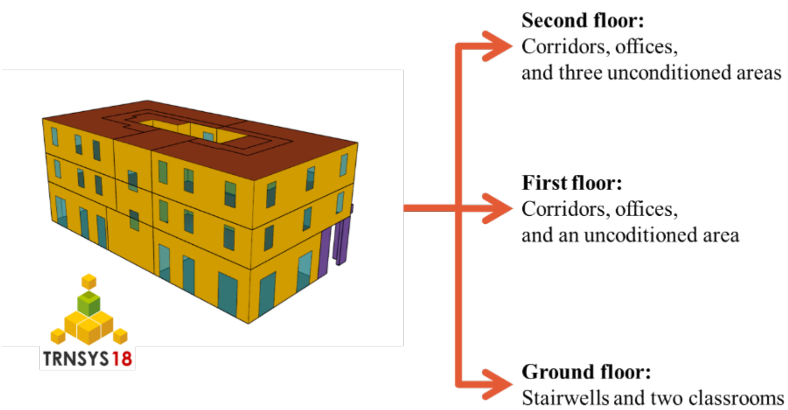

Figure 1. Building model.

The storage tank is modeled using Type 158, with temperature control managed by Type 106 thermostats during the heating season and Type 113 thermostats during the cooling season. A heating set-point of 47°C is defined for Type 106, while a cooling set-point of 12°C is defined for Type 113. The circulation pumps are represented using Type 110, which operates at a constant flow rate corresponding to the nominal value. Finally, the EHP is modeled using Type 525 from the TESS additional library [25]. This component allows the compressor speed to be modulated to maintain a constant fluid outlet temperature despite variations in inlet water temperature and ambient conditions. The outlet water set-point temperature is specified as an input to Type 525 and is equal to 49°C during the heating season and 10°C during the cooling season. Additionally, this component requires a performance map based on data provided in the manufacturer's datasheet [23].

2.3. Environmental impact assessment

As outlined in the Introduction, the ETEWI index represents an extension of the conventional TEWI metric. This index is computed as the sum of multiple contributions: the direct effect of refrigerant leakages into the atmosphere ($TEWI_{dir}^{RL}$), the direct impact of the UHI phenomenon ($TEWI_{dir}^{UHI}$), the indirect contribution associated with the power grid (PG, $TEWI_{ind}^{PG}$), the indirect impact of transmission and distribution (TD) losses in natural gas pipelines ($TEWI_{ind}^{TD}$), and the indirect effect of UHI ($TEWI_{ind}^{UHI}$). In the present work, the direct contribution from fuel combustion is not considered, as no combustion-based systems are included in the analyzed case study. The ETEWI formulation is presented in Eq. (1).

$$ETEWI = TEWI_{dir}^{RL} + TEWI_{dir}^{UHI} + TEWI_{ind}^{PG} + TEWI_{ind}^{TD} + TEWI_{ind}^{UHI} \quad (1)$$

Both the direct and indirect TEWI components ($TEWI_{dir}^{RL}$ and $TEWI_{ind}^{PG}$) are refined by incorporating dynamic values for refrigerant leakages, electricity demand of the plant, and the equivalent carbon dioxide (CO_{2eq}) emission factor of the PG.

For the direct component, $TEWI_{dir}^{RL}$, a dynamic approach is employed to quantify refrigerant leakages (RL) on a monthly basis throughout the plant's operational lifetime and account for refrigerant refilling. Specifically, $TEWI_{dir}^{RL}$ is calculated as described in Eq. (2), where the total refrigerant losses over the plant lifetime are obtained by summing the monthly leakages across all n operating months. In this equation, GWP denotes the global warming potential of the refrigerant, $AdpGWP$ represents the GWP of the refrigerant's atmospheric degradation product, C is the refrigerant charge, and EOL refers to the end-of-life leakage occurring during the disposal of the EHP. The end-of-life refrigerant losses are quantified considering the final charge of refrigerant, since C_n corresponds to refrigerant charge calculated in the last operating month. The effect of refrigerant refilling operations is also accounted for. This contribution is evaluated as the sum, over all m refilling events, of the actual refrigerant charge at the j-th maintenance operation (C_j), multiplied by EOL. Each monthly leakage (RL_i), is determined according to Eq. (3), where ALR denotes the annual leakage ratio of the refrigerant, and L represents the expected lifetime of the plant. Table 4 provides a summary of the values of all parameters adopted in Eqs. (2) and (3).

$$TEWI_{dir}^{RL} = (GWP + AdpGWP) \cdot \left[\sum_{i=1}^{n} RL_i + C_n \cdot EOL + \sum_{j=1}^{m} C_j \cdot EOL \right] \quad (2)$$

$$RL_i = C_{(i-1)} \cdot \frac{ALR}{(n/L)} \quad (3)$$

Table 3. Parameters for ETEWI evaluation.

Parameter	Value	Reference
L [y]	15	[26]
ALR [y^{-1}]	0.025	[26]
EOL [-]	0.15	[26]
GWP [$kgCO_{2eq}/kg$]	2088	[21]
$AdpGWP$ [$kgCO_{2eq}/kg$]	Not available	[26]

The term $TEWI_{dir}^{UHI}$ represents the direct contribution of the UHI effect. This contribution is evaluated using an exergy-based approach, as expressed in Eq. (4). The time-dependent evaluation of $TEWI_{dir}^{UHI}$, which is conducted on an hourly basis, accounts for all operating hours over the plant lifetime (θ_{end}). The hourly CO_{2eq} emission factor of the PG, $\alpha(\theta)$, refers to electricity production in Italy during 2022 [27]. The term $\tau^{UHI}(\theta)$ denotes the hourly dimensionless exergetic temperature, while $E_{co}^{EHP,CD}(\theta)$ represents the condenser heat discharged to the atmosphere during summer operation on an hourly basis. According to Eq. (5), $\tau^{UHI}(\theta)$ is evaluated considering $T_{UHI}(\theta)$, the outdoor air temperature measured in the urban area of Benevento in 2022. This temperature was compared with measurements from a suburban area unaffected by UHI effects [28], revealing an average urban temperature increase of 4.3 K. This difference was used to calculate the hourly base temperature $T_0(\theta)$.

$$TEWI_{dir}^{UHI} = \sum_{\theta=0}^{\theta_{end}} (\alpha(\theta) \cdot \tau^{UHI}(\theta) \cdot E_{co}^{EHP,CD}(\theta)) \tag{4}$$

$$\tau^{UHI}(\theta) = 1 - \frac{T_0(\theta)}{T_{UHI}(\theta)} \tag{5}$$

The term $TEWI_{ind}^{PG}$ is dynamically evaluated using the hourly electric load of the plant including auxiliaries ($E_{el}^{HVAC}(\theta)$), as indicated in Eq. (6). $TEWI_{ind}^{UHI}$ is neglected because the influence of increased temperature on EHP performance and electricity demand is already captured within $TEWI_{ind}^{PG}$. In fact, $E_{el}^{HVAC}(\theta)$ is estimated through dynamic yearly simulations using the temperature data in the urban area of Benevento as input data in the building-plant system model, inherently reflecting UHI effects. Finally, $TEWI_{ind}^{TD}$ is assessed as described in Eq. (7). Here, V_{NGL} denotes the total volume of natural gas losses (NGL) due to TD leakages over the EHP's lifetime, $\overline{GWP}_{mix,NG}$ is the global warming potential of natural gas, and $\bar{\rho}_{mix,NG}$ is its density [29]. The total NGL volume is calculated assuming a TD leakage coefficient of 0.85% of the total natural gas used for supplying E_{el}^{HVAC}. Specifically, the contribution of each electricity production unit to the total electricity production mix is known on an hourly basis; consequently, the electricity production share attributable to natural gas-fired thermoelectric plants is also known. The hourly share of $E_{el}^{HVAC}(\theta)$ supplied by natural gas-fired thermoelectric plants is used to calculate the corresponding primary energy demand, considering an energy conversion efficiency of 0.561 in 2022 [30]. The resulting primary energy demand is then employed to estimate the total volume of natural gas needed and the related leakages.

$$TEWI_{ind}^{PG} = \sum_{\theta=0}^{\theta_{end}} \alpha(\theta) \cdot E_{el}^{HVAC}(\theta) \tag{6}$$

$$TEWI_{ind}^{TD} = V_{NGL} \cdot \overline{GWP}_{mix,NG} \cdot \bar{\rho}_{mix,NG} \tag{7}$$

As previously mentioned, the environmental impact assessment of the case study under analysis is carried out based on the results obtained from dynamic simulations performed with a 1.5-minute timestep in TRNSYS 18. The building-plant model uses as input temperature data collected in 2022 in the urban area of Benevento with a 15-minute time step, referred to as T_{UHI}. These data are used to estimate the building's heating and cooling loads, as well as the performance of the air-source EHP, according to manufacturer's datasheet (which is used to construct the input performance maps). Figure 2 shows the trend of the measured temperature.

The temperature data collected in 2022 are also employed to develop a forward-looking analysis aimed at assessing the variations in heating, cooling, and electricity loads expected in future decades due to climate change. In this regard, six scenarios are evaluated in this work, each characterized by a specific temperature increase (ΔT) compared to the baseline temperature measured in 2022:

- Scenario #0: based on the simulation using the actual temperature measured in Benevento ($\Delta T =$ 0 °C).
- Scenario #1: actual 2022 temperature increased by 1°C.
- Scenario #2: actual 2022 temperature increased by 2°C.
- Scenario #3: actual 2022 temperature increased by 3°C
- Scenario #4: actual 2022 temperature increased by 4°C
- Scenario #5: actual 2022 temperature increased by 5°C.

The simulations are performed for each scenario, considering a one-year period and the corresponding ΔT increase. The environmental analysis is then carried out over a 15-year operational period of the EHP. It is assumed that, during each year of operation, the system behaves as in the reference year of the simulation.

Hence, the building maintains the same annual heating and cooling loads, and the EHP exhibits the same annual electric load throughout its entire lifetime. Similarly, the data regarding $\alpha(\theta)$, $T_{UHI}(\theta)$, and V_{NGL} used to calculate $TEWI_{dir}^{UHI}$, $TEWI_{ind}^{PG}$ and $TEWI_{ind}^{T\&D}$ correspond to the year 2022 for each analysed year.

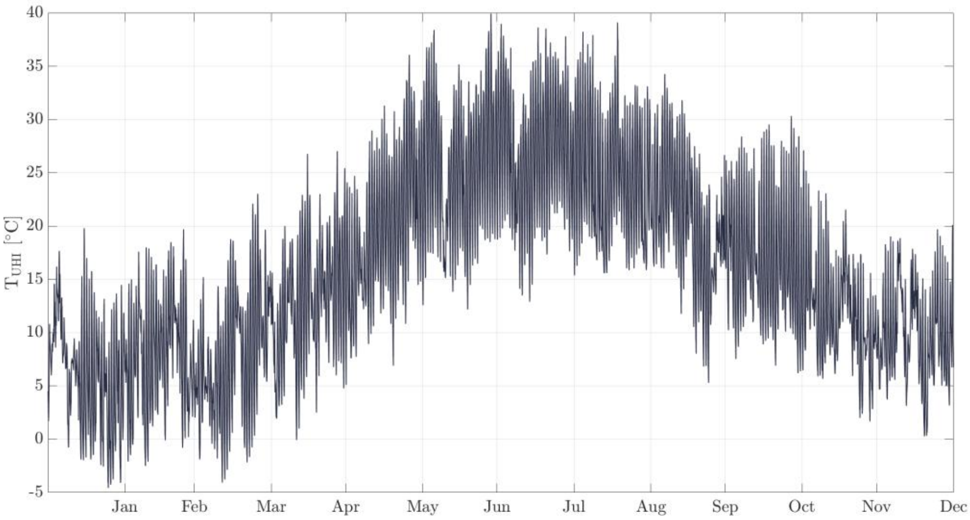

Figure 2. Temperature data in the urban area of Benevento (2022).

3. Results and Discussion

Figure 3(a) shows the trend of the thermal and cooling energy supplied by the EHP across the analyzed scenarios, considering the increasing ΔT. Overall, the total energy supplied remains almost constant, while the heating energy decreases and the cooling energy increases. Specifically, in heating mode, the EHP supplies 83.8 MWh/y in scenario #0 (with ΔT equal to 0°C) and 48.7 MWh/y in scenario #5 (with ΔT equal to 5°C). Conversely, the cooling energy supplied by the EHP increases from 22.9 to 56.3 MWh/y over the same scenarios. Correspondingly, the electric load of the EHP remains nearly constant across the scenarios, although the seasonal loads vary significantly depending on the ΔT considered (Figure 3(b)). In scenario #0, the electric energy demand of the EHP is 27.6 MWh/y in heating mode and 8.2 MWh/y in cooling mode. In scenario #5, the EHP requires 14.4 MWh/y in heating mode and 21.4 MWh/y in cooling mode. These results indicate that increasing temperature trends will significantly affect building heating and cooling loads, thereby intensifying the electric energy demand of buildings during the summer period.

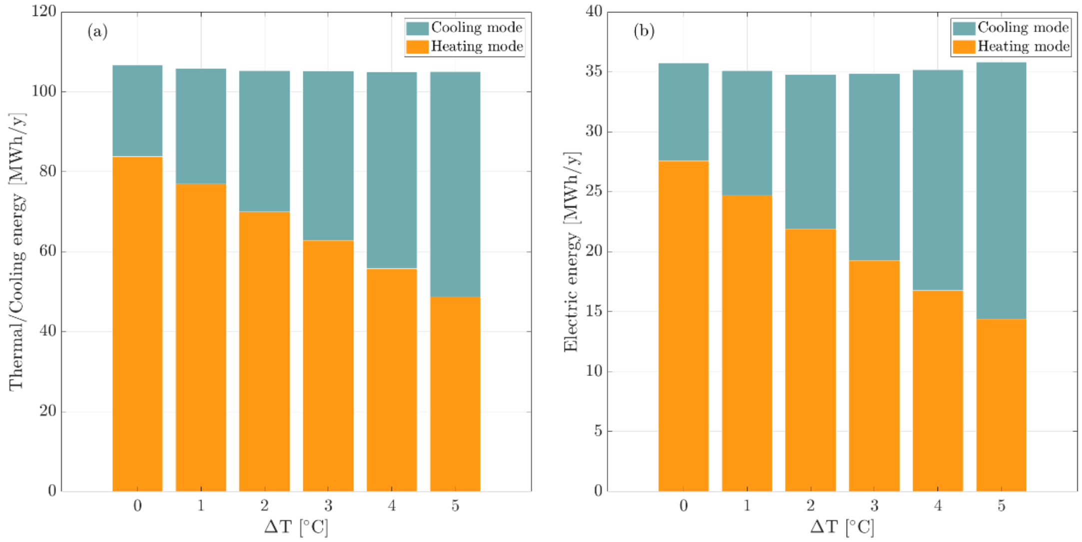

Figure 3. Thermal/cooling energy supplied by the EHP across investigated scenarios (a).
Electric energy required by the EHP across investigated scenarios (b).

In summer, due to the increasing cooling loads, the thermal energy released by the EHP condenser rises, too. The results obtained from the simulations with increasing ΔT are summarized in Figure 4. The heat released by the condenser increases drastically across the scenarios, from 31.1 MWh/y with ΔT equal to 0°, to 77.7 MWh/y with ΔT equal to 5°C. These findings highlight the challenges and key considerations associated with recognizing EHPs as enabling technologies for the decarbonization of the heating and cooling sectors. The effectiveness of these systems is closely tied to the possibility of integrating them with renewable-based plants. However, this integration improves their sustainability only by reducing dependance on fossil-based electricity production mixes. Other potential indirect impacts should also be examined, and the indirect contribution to greenhouse gas emissions resulting from the exacerbation of the UHI phenomenon, which is far from negligible (especially in future years expected to be characterized by rising outdoor temperatures) should be carefully considered.

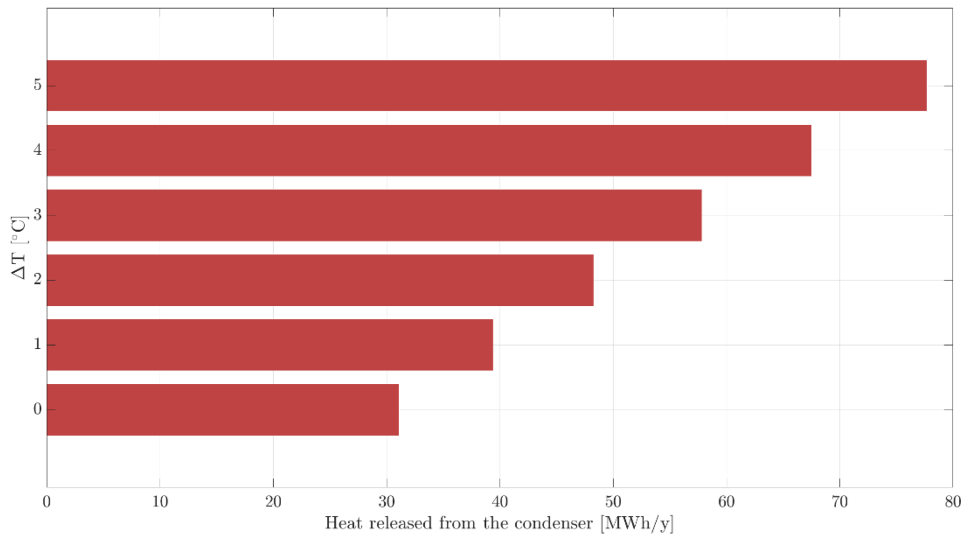

Figure 4. Heat released from the condenser across investigated scenarios.

The results obtained from the environmental impact analysis are summarized in Table 4. Across the scenarios, the indirect contribution due to the PG ($TEWI_{ind}^{PG}$) shows a decreasing trend, from 207.5 tCO_{2eq} in scenario #0 to 198.1 tCO_{2eq} in scenario #1. This outcome is particularly relevant, as it indicates that increasing temperature trends will lead to greater EHP operation during the summer, when the CO_{2eq} emission factor of the PG is generally lower due to the higher penetration of renewables in the electricity production mix. The term $TEWI_{ind}^{TD}$ decreases, too, as the share of electric energy supplied by natural gas-fired power plants is lower during the summer. Conversely, an increasing contribution is observed in $TEWI_{dir}^{UHI}$, which rises due to the greater heat released by the EHP condenser operating in cooling mode, as previously discussed. Although it represents only a small fraction of the total $ETEWI$, its share grows across scenarios (Figure 5): 1.89% in scenario #0, 2.39% in scenario #1, 2.92% in scenario #2, 3.47% in scenario #3, 4.04% in scenario #4, 4.62% in scenario #5. While this contribution is limited, it highlights potential drawbacks associated with increasing cooling energy demand in buildings served by EHPs. These effects may be more pronounced when certain limitations of this study are addressed:

- with rising temperatures, reflected by decreasing heating degree days and increasing cooling degree days, the activation periods of heating, ventilation, air conditioning, and refrigeration systems will change. In this study, the activation period of the EHP is assumed to remain constant to ensure compliance with the existing Italian regulatory framework. Shorter heating periods would further reduce heating energy demand, whereas longer cooling periods would increase cooling demand. Consequently, the direct environmental impact of EHPs affecting the UHI phenomenon will also change accordingly.
- The temperature increases considered in the various scenarios are intended only as examples of the potential effects of rising temperature trends, which may be more pronounced and unevenly distributed throughout the year, thereby affecting the total heating and cooling loads of the building in ways not fully captured by the current assumptions.
- In the present case study, the EHP operates according to the building's occupancy schedule and is therefore turned off at night. Although rising temperatures may also affect nighttime thermal comfort, this aspect is not captured in the current research, as the selected building is occupied only during daytime hours. Preliminary findings indicate an increasing contribution of $TEWI_{dir}^{UHI}$, which would be even higher if longer daily operating hours were assumed for buildings with continuous heating and cooling demands, such as residential buildings and hotels.
- In this research, the effect of performance degradation of the EHP over its lifetime is not considered. However, reduced performance increases the plant's electric load, thereby further exacerbating both the direct and indirect impacts of the UHI phenomenon on total greenhouse gas emissions.

Based on these considerations, this study may serve as the basis for highlighting the importance of accounting for the UHI effect when evaluating the environmental impact of electric-driven energy conversion systems such as EHPs. On the one hand, the ongoing decarbonization of the PG helps reduce the indirect impact associated with the electricity demand for their operation. Likewise, the adoption of low-GWP refrigerants can mitigate the direct environmental impact of these systems. However, a comprehensive environmental assessment should also consider the indirect contribution of EHPs to climate change through their role in exacerbating the UHI effect in urban areas. In this context, the $ETEWI$ index proves to be a valuable tool, as it captures these phenomena and ensures they are adequately addressed in decarbonization strategies driven by the electrification of the heating and cooling sectors.

Table 4. Results of environmental impact assessment.

Scenario	ΔT [°C]	$TEWI_{dir}^{RL}$ [tCO_{2eq}]	$TEWI_{dir}^{UHI}$ [tCO_{2eq}]	$TEWI_{ind}^{PG}$ [tCO_{2eq}]	$TEWI_{ind}^{TD}$ [tCO_{2eq}]	$ETEWI$ [tCO_{2eq}]
#0	0	66.0	1.89	207.5	12.4	287.8
#1	1	66.0	2.39	202.8	12.0	283.2
#2	2	66.0	2.92	200.4	11.9	281.2
#3	3	66.0	3.47	198.6	11.7	279.8
#4	4	66.0	4.04	197.7	11.6	279.3
#5	5	66.0	4.63	198.1	11.5	280.2

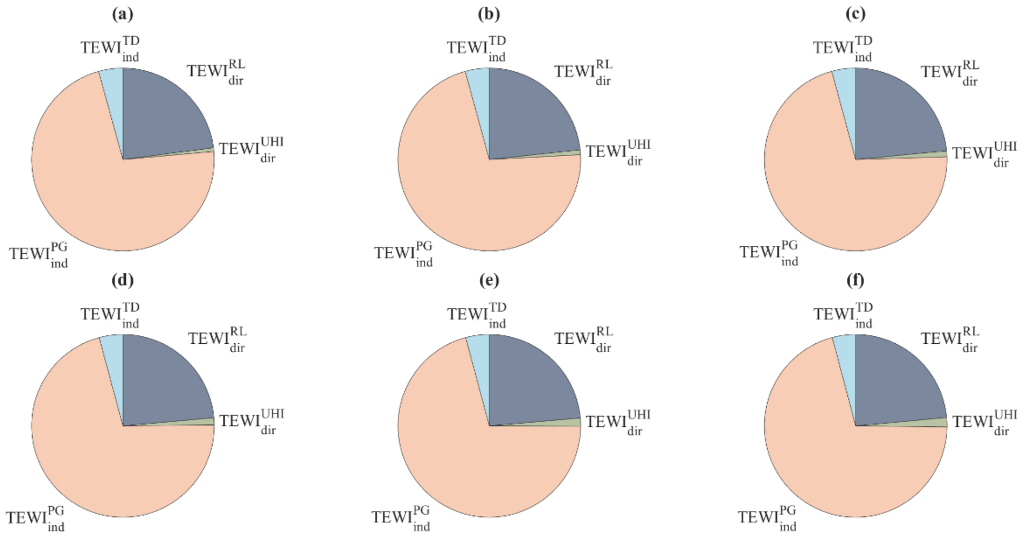

Figure 5. Distribution of ETEWI contributions in scenario #0 (a), scenario #1 (b), scenario #2 (c), scenario #3 (d), scenario #4 (e), and scenario #5 (f).

4. Conclusions

This study investigates the environmental impact of an air-to-water, electric-driven heat pump installed in a historic university building located in Benevento, southern Italy. The analysis is based on the results of dynamic simulations that use temperature data collected in the city's urban area in 2022. These data are subsequently modified by increasing temperature levels from 1 to 5 °C in order to perform new simulations assessing the effects of rising temperatures on the building's heating and cooling loads, the heat pump's performance, and its overall environmental impact. To this end, the Expanded Total Equivalent Warming Impact (ETEWI) index is calculated.

The results show that rising temperatures significantly affect the building's heating and cooling loads. Specifically, the heating energy demand decreases, while the cooling demand increases markedly as temperature rises; however, their combined total remains nearly constant across the analyzed scenarios. Consequently, the electric load of the heat pump remains relatively stable on an annual basis, although it shifts seasonally, with higher electricity consumption during the summer months. Moreover, because of the increased cooling load, the heat discharged by the condenser when the heat pump operates in cooling mode also rises with temperature, thereby contributing to the intensification of the urban heat island effect.

The environmental impact analysis using the ETEWI index reveals that the indirect environmental impact of the electric heat pump, associated with the electricity taken from the power grid for its operation, decreases slightly due to the shift in operation from winter to summer, when the share of renewables in the electricity mix is higher. In contrast, the direct contribution linked to the urban heat island effect rises with increasing temperature. While this contribution represents only a small portion of the total ETEWI, it exhibits a consistent upward trend across the analyzed scenarios, underscoring the potential long-term impacts of increasing cooling demands in urban environments. These findings underline the importance of integrating the urban heat island phenomenon into environmental assessments of electric-driven heat pumps for heating and cooling energy supply in buildings. Although decarbonization of the electricity mix and adoption of low-global warming potential refrigerants can reduce traditional indirect and direct impacts, overlooking the exacerbation of local urban warming may lead to underestimating the overall environmental footprint of heat pump deployment in cities.

Overall, this work demonstrates that the ETEWI index is an effective tool for capturing comprehensively the environmental impact of electric heat pumps under evolving climatic conditions. Accounting for the urban heat island effect is essential for designing sustainable electrification strategies in the heating and cooling sector, particularly in urban areas expected to experience more pronounced warming in the coming decades.

Future studies should consider variable occupancy schedules, longer operational hours, and more detailed climate projections to further refine these assessments.

Nomenclature

Acronyms and abbreviations

CO_{2eq}	Equivalent Carbon Dioxide
EHP	Electric Heat Pump
LCCP	Life Cycle Climate Performance
NGL	Natural Gas Leakage
PG	Power Grid
TD	Transmission and Distribution
TEWI	Total Equivalent Warming Impact
UHI	Urban Heat Island

Symbols

ΔT	Temperature lift [°C]
$AdpGWP$	Atmospheric degradation product global warming potential [$kgCO_{2eq}/kg$]
ALR	Annual leakage ratio [-]
C	Refrigerant charge [kg]
COP	Coefficient of performance [-]
E_{co}^{EHP}	Thermal energy released by the EHP condenser in cooling mode [MWh/y]
E_{el}^{HVAC}	Electric energy demand of the plant [MWh/y]
EER	Energy efficiency ratio [-]
EOL	End of life [-]
$ETEWI$	Expanded Total Equivalent Warming Impact [tCO_{2eq}]
GWP	Global Warming Potential [$kgCO_{2eq}/kg$]
n	Number of operating months [-]
RL	Refrigerant Leakage [kg]
T_0	Base air temperature [°C]
T_{UHI}	Urban air temperature [°C]
$TEWI_{dir}^{RL}$	Direct contribution of refrigerant leakages [tCO_{2eq}]
$TEWI_{dir}^{UHI}$	Direct contribution of the urban heat island phenomenon [tCO_{2eq}]
$TEWI_{ind}^{PG}$	Indirect contribution of the power grid [tCO_{2eq}]
$TEWI_{ind}^{TD}$	Indirect contribution of transmission and distribution losses [tCO_{2eq}]
$TEWI_{ind}^{UHI}$	Indirect contribution of the urban heat island phenomenon [tCO_{2eq}]
V_{NGL}	Total volume of natural gas leakages [m^3]

Greek letters and subscripts

α	Equivalent carbon dioxide emission factor for electricity production [$kgCO_{2eq}/kWh_{el}$]
θ	Hourly timestep [-]
ρ	Density [kg/m^3]
τ^{UHI}	Dimensionless exergetic temperature [-]
NG	Natural gas
mix	Electricity production mix

Acknowledgements

This work was supported by the thematic table "Attività produttive per contribuire al conseguimento di elevati livelli di occupazione, all'adattamento dei lavoratori, delle imprese e degli imprenditori ai cambiamenti, e all'accrescimento della competitività e dello sviluppo economico", CUP F85E25000100006– SURF 23097AP000000008, funded by Regione Campania within the 2021–2027 programming of the PR Campania FSE+ and PR Campania FESR

References

[1] G. Buster, J. Cox, B. N. Benton, and R. N. King, "Estimating the impacts of increasing temperatures and the efficacy of climate adaptation strategies in urban microclimates with deep learning," *Urban Clim*, vol. 64, p. 102603, Dec. 2025, doi: 10.1016/j.uclim.2025.102603.

[2] United Nations, "World Urbanisation Prospects 2018," 2018. Accessed: Oct. 28, 2025. [Online]. Available:

https://population.un.org/wup/.
[3] D. Zhou, J. Xiao, S. Frolking, L. Zhang, and G. Zhou, “Urbanization Contributes Little to Global Warming but Substantially Intensifies Local and Regional Land Surface Warming,” *Earths Future*, vol. 10, no. 5, May 2022, doi: 10.1029/2021EF002401.
[4] L. M. A. Bettencourt, J. Lobo, D. Helbing, C. Kühnert, and G. B. West, “Growth, innovation, scaling, and the pace of life in cities,” *Proceedings of the National Academy of Sciences*, vol. 104, no. 17, pp. 7301–7306, Apr. 2007, doi: 10.1073/pnas.0610172104.
[5] L. Zhao *et al.*, “Global multi-model projections of local urban climates,” *Nat Clim Chang*, vol. 11, no. 2, pp. 152–157, Feb. 2021, doi: 10.1038/s41558-020-00958-8.
[6] V. Sangiorgio, F. Fiorito, and M. Santamouris, “Development of a holistic urban heat island evaluation methodology,” *Sci Rep*, vol. 10, no. 1, p. 17913, Oct. 2020, doi: 10.1038/s41598-020-75018-4.
[7] A. Mohajerani, J. Bakaric, and T. Jeffrey-Bailey, “The urban heat island effect, its causes, and mitigation, with reference to the thermal properties of asphalt concrete,” *J Environ Manage*, vol. 197, pp. 522–538, Jul. 2017, doi: 10.1016/j.jenvman.2017.03.095.
[8] S. Guarino, A. Buscemi, M. Bonomolo, M. Beccali, and V. Lo Brano, “Low-carbon heating solutions using road thermal collectors and seasonal energy storage in mediterranean climates,” *Energy Conversion and Management: X*, vol. 27, p. 101167, Jul. 2025, doi: 10.1016/j.ecmx.2025.101167.
[9] L. Sheng *et al.*, “Effect analysis on thermal profile management of a cylindrical lithium-ion battery utilizing a cellular liquid cooling jacket,” *Energy*, vol. 220, p. 119725, Apr. 2021, doi: 10.1016/j.energy.2020.119725.
[10] Y. Hu, B. Shen, H. Wan, K. R. Gluesenkamp, S. Krishnamoorthy, and D. Shirey, “Heating performance of a vapor compression heat pump cascaded with a thermoelectric heat pump,” *Appl Therm Eng*, vol. 249, p. 123397, Jul. 2024, doi: 10.1016/j.applthermaleng.2024.123397.
[11] J. Volt, A. Toleikyte, J. C. Roca Reina, A. Mountraki, and S. Letout, “Clean Energy Technology Observatory: Heat Pumps in the European Union - 2025 Status Report on Technology Development, Trends, Value Chains and Markets,” Luxembourg, 2025. Accessed: Jan. 13, 2026. [Online]. Available: https://data.europa.eu/doi/10.2760/3976212.
[12] X. Li, Y. Zhou, S. Yu, G. Jia, H. Li, and W. Li, “Urban heat island impacts on building energy consumption: A review of approaches and findings,” *Energy*, vol. 174, pp. 407–419, May 2019, doi: 10.1016/j.energy.2019.02.183.
[13] L. Shi, Z. Luo, W. Matthews, Z. Wang, Y. Li, and J. Liu, “Impacts of urban microclimate on summertime sensible and latent energy demand for cooling in residential buildings of Hong Kong,” *Energy*, vol. 189, p. 116208, Dec. 2019, doi: 10.1016/j.energy.2019.116208.
[14] R. Sun, Y. Wang, and L. Chen, “A distributed model for quantifying temporal-spatial patterns of anthropogenic heat based on energy consumption,” *J Clean Prod*, vol. 170, pp. 601–609, Jan. 2018, doi: 10.1016/j.jclepro.2017.09.153.
[15] M. Ferrando, T. Hong, and F. Causone, “A simulation-based assessment of technologies to reduce heat emissions from buildings,” *Build Environ*, vol. 195, p. 107772, May 2021, doi: 10.1016/j.buildenv.2021.107772.
[16] C. Guattari, L. Evangelisti, and C. A. Balaras, “On the assessment of urban heat island phenomenon and its effects on building energy performance: A case study of Rome (Italy),” *Energy Build*, vol. 158, pp. 605–615, Jan. 2018, doi: 10.1016/j.enbuild.2017.10.050.
[17] V. Q. Doan, H. Kusaka, and T. M. Nguyen, “Roles of past, present, and future land use and anthropogenic heat release changes on urban heat island effects in Hanoi, Vietnam: Numerical experiments with a regional climate model,” *Sustain Cities Soc*, vol. 47, p. 101479, May 2019, doi: 10.1016/j.scs.2019.101479.
[18] S. K. Fischer, “Total equivalent warming impact: a measure of the global warming impact of CFC alternatives in refrigerating equipment,” *International Journal of Refrigeration*, vol. 16, no. 6, pp. 423–428, Jan. 1993, doi: 10.1016/0140-7007(93)90059-H.
[19] United Nations Environment Programme, “The implications to the Montreal Protocol of the inclusion of HFC and PFCs in the Kyoto Protocol,” 199AD, Accessed: Oct. 28, 2025. [Online]. Available: https://ozone.unep.org/sites/default/files/2019-05/HFCPFC.pdf.
[20] F. Ceglia, E. Marrasso, C. Roselli, and M. Sasso, “An innovative environmental parameter: Expanded Total Equivalent Warming Impact,” *International Journal of Refrigeration*, vol. 131, pp. 980–989, Nov. 2021, doi: 10.1016/j.ijrefrig.2021.08.019.
[21] F. Ceglia, E. Marrasso, C. Martone, G. Pallotta, C. Roselli, and M. Sasso, “Environmental impact assessment of an air-to-water heat pump through the expanded total equivalent warming impact index based on experimental data,” *International Journal of Refrigeration*, vol. 155, pp. 305–319, Nov. 2023, doi: 10.1016/j.ijrefrig.2023.08.020.
[22] Gazzetta Ufficiale della Repubblica Italiana, “Decreto del Presidente della Repubblica 26 Agosto 1993, n. 412, Regolamento recante norme per la progettazione, l’installazione, l’esercizio e la manutenzione degli impianti termici degli edifici ai fini del contenimento dei consumi di energia, in attuazione dell’art. 4, comma 4, della legge 9 gennaio, 10.”
[23] AERMEC S.p.A., “Technical booklet Aermec NRL1000 Reversible air-to-water heat pump for outdoor installation,” 2022. Accessed: Oct. 28, 2025. [Online]. Available: https://global.aermec.com/it/products/.
[24] S.A. Klein, “TRNSYS 18: a transient system simulation program,” Madison, USA, 2017. Accessed: Aug. 02, 2025. [Online]. Available: http://sel.me.wisc.edu/trnsys
[25] Thermal Energy System Specialists (TESS), “TESS component library.” Accessed: Aug. 02, 2025. [Online]. Available: https://www.trnsys.com/tess-libraries/GeneralDescriptions_TESSLibs18.pdf.
[26] International Institute of Refrigeration, “Harmonization of Life Cycle Climate Performance Methodology,” 2016. Accessed: Oct. 28, 2025. [Online]. Available: https://iifiir.org/en/fridoc/harmonization-of-life-cycle-climate-performance-methodology-139940.
[27] F. Ceglia, E. Marrasso, C. Roselli, and M. Sasso, “Time-evolution and forecasting of environmental and energy performance of electricity production system at national and at bidding zone level,” *Energy Convers Manag*, vol. 265, Aug. 2022, doi: 10.1016/j.enconman.2022.115772.
[28] CEntro MEteorologico e Climatologico, “Pubblicazione dati grezzi dei sensori meteo della Rete di Monitoraggio della Qualità dell’aria,” 2023. Accessed: Oct. 28, 2025. [Online]. Available: https://cemec.arpacampania.it/misure_suolo.php.
[29] SNAM, “Il Metanino, 2019 Dati statistici ,” 2019. Accessed: Oct. 28, 2025. [Online]. Available: https://www.snam.it/export/sites/snam-rp/repository/file/investor_relations/aggiornamenti_azionisti/Metanino/metanino_2019_ita.pdf.
[30] Terna, “Produzione,” 2023. Accessed: Oct. 28, 2025. [Online]. Available: https://www.terna.it/it/sistema-elettrico/statistiche/pubblicazioni-statistiche.